Available online at www.sciencedirect.com
ScienceDirect
Journal of Power Sources 161 (2006) 282–289
JOURNAL OF POWER SOURCES
www.elsevier.com/locate/jpowsour

Advanced air-breathing direct methanol fuel cells for portable applications

Y.H. Pan *

Tekion Inc., MEA Development, 60 Hazelwood Drive, Champaign, IL 61820, United States

Received 25 February 2006; received in revised form 26 March 2006; accepted 28 March 2006
Available online 4 May 2006

Abstract

A novel MEA is fabricated to improve the performance of air-breathing direct methanol fuel cells. A diffusion barrier on the anode side is designed to control methanol transport to the anode catalyst layer and thus suppressing the methanol crossover. A catalyst coated membrane with a hydrophobic gas diffusion layer on the cathode side is employed to improve the oxygen mass transport. It is observed that the maximum power density of the advanced DMFC with 2 M methanol solution achieves 65 mW cm^{-2} at 60 °C. The value is nearly two times more than that of a commercial MEA. At 40 °C, the power densities operating with 1 and 2 M methanol solutions are over 20 mW cm^{-2} with a cell potential at 0.3 V.

Keywords: Direct methanol fuel cells

1. Introduction

The direct methanol fuel cell (DMFC) is a promising power source for portable applications due to its high energy density, long life, and no need for charging. Extensive efforts have been carried out to develop advanced DMFC technology to meet commercial requirements. However, much research has been directed toward the DMFC operated with forced air flow at relatively high temperatures (>80 °C) [1–3], some operated higher than 100 °C (vapor-feed systems) [4–6] to obtain better performance. High temperatures tend to increase methanol crossover and reduce efficiency due to additional energy required to evaporate the aqueous methanol fuel. It may not be practical to operate the fuel cell system at high temperature for portable applications. In addition, the air pump or compressed air reservoir decreases achievable energy density and power density due to extra power and/or space requirement for fuel cell systems.

In order to miniaturize the fuel cell systems, it is highly desired to operate the air cathode passively (air-breathing direct methanol fuel cell) at room temperature. Compared with a forced convection air cathode, an air-breathing cathode is required to remove water (gas and liquid) and supply air more efficiently. It is found that a cathode, made by catalyst directly coated onto a membrane with a hydrophobic carbon cloth gas diffusion layer (GDL), achieves desired results [7]. Based on previous studies [7,9], a novel MEA is fabricated to accomplish further progress.

2. Experimental

All anodes employed in this research were fabricated by the same method as described in the previous study [7,9]. There were two kinds of cathodes in this research: in-house cathode based on carbon paper with a micro-porous layer and a catalyst coated membrane (CCM) cathode made by ion power. A commercial carbon cloth-backing layer (Single side Elat® purchased from E-tek) served as the GDL for CCM cathode. It is known that there are two types of catalyst layer fabrication processes: catalyst coated on the backing layer (either carbon paper with/without micro-porous layer or carbon cloth with/without micro-porous layer) and catalyst coated directly on the polymer electrolyte membrane (CCM). The fabrication process of the novel MEA is plotted in Fig. 1. It can be seen that the cathode catalyst layer is coated on the membrane and the anode catalyst is coated on the backing layer. The catalyst coated membrane was placed in the middle of the anode and the cathode GDL (projected surface area 5 cm^2) and then hot pressed to form the MEA at 125 °C and 100 kg cm^{-2} for 3 min.

* Tel.: +1 217 328 9852; fax: +1 217 333 4050.
E-mail address: ypan@tekion.com.

0378-7753/$ – see front matter © 2006 Elsevier B.V. All rights reserved.
doi:10.1016/j.jpowsour.2006.03.048

Nomenclature

c	molar concentration (mol l^{-1})
D	diffusivity (cm^2 s^{-1})
E	electrode potential (V)
E^{eq}	thermodynamic equilibrium potential (V)
F	Faraday's constant, 96485 C mol^{-1}
g	gravitational acceleration (m s^{-2})
ΔG°	standard Gibbs free energy change (kJ mol^{-1})
h	Meniscus height (m)
ΔH°	standard Gibbs free energy change (kJ mol^{-1})
i	current density (mA cm^{-2})
i_{cross}	methanol crossover current density (mA cm^{-2})
i_0	exchange current density (mA cm^{-2})
J	molar flux (mol cm^{-2} s)
l	thickness of layer (cm)
n_d	electro-osmotic drag coefficient
R	gas constant (8.314 J mol^{-1} K^{-1})

Greek letters

α	transfer coefficient
η	overpotential (V)
η_{eff}	theoretical thermodynamic efficiency
θ	contact angle (°)
ρ	density (kg m^{-3})
σ	surface tension (N cm^{-1})

Superscripts

MeOH	methanol
O_2	oxygen
oc	open circuit

Subscripts

a	anode
b	anode backing layer
c	cathode
cross	methanol crossover
eff	effective value
lim	limiting current density
m	membrane

The forced convection fuel cell hardware was the same used in the previous study [7,9]; a stainless steel plate with two 5 cm^2 (shown in the Fig. 2) parallel style flow fields that have a 1 mm channel width and a 0.5 mm rib width. A layer of gold was deposited on the inner surface of the end plate. However, a new designed air-breathing hardware (shown in Fig. 3) for the cathode side was applied. It includes two parts: the first is a current collector with a parallel field, 1 mm channel width, 0.5 mm rib width, and a gold coating layer on the surface contacting with MEA; the second is a backing end plate with an open square window that allows air to pass through freely. The fuel cell was operated at 25 (ambient temperature), 40, and 60 °C, and the electrochemical tests were controlled by an Arbin BT + 4 Testing System. The methanol solutions were pumped through the flow field by a peristaltic pump (Omega) with the same flow rate of 0.2 ml s^{-1} and without backpressure. Polarization curves were measured by a galvanodynamic polarization mode at the scan rate of 3 mA s^{-1}.

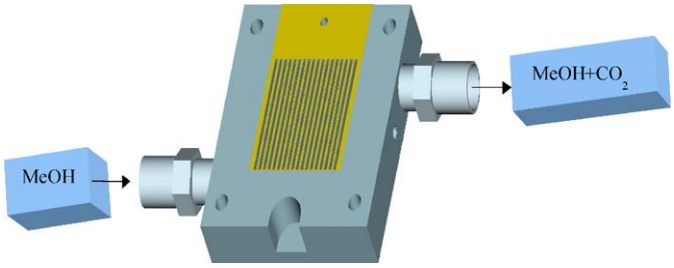

Fig. 2. Schematic diagram of the anode flow field of stainless steel plates.

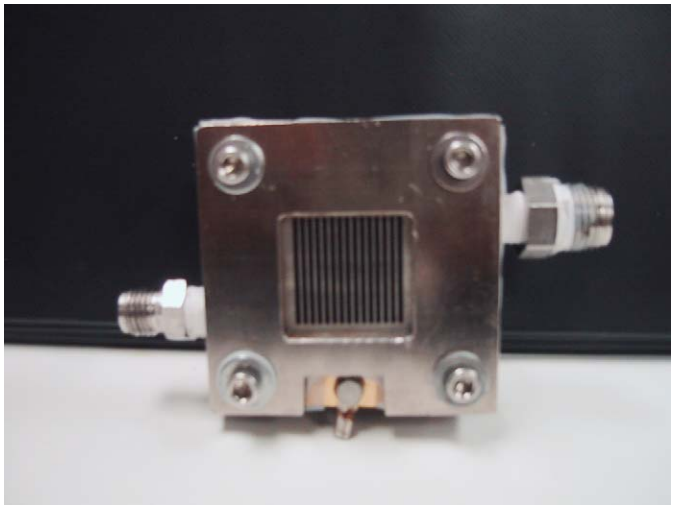

Fig. 3. Picture of an air-breathing fuel cell.

3. Results and discussion

3.1. Theoretical analysis of methanol transport

Although theoretical thermodynamic efficiency of direct methanol fuel cells is very high, crossover of methanol from

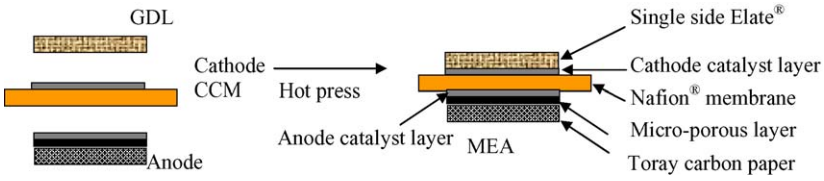

Fig. 1. Schematic diagram of MEA fabrication process.

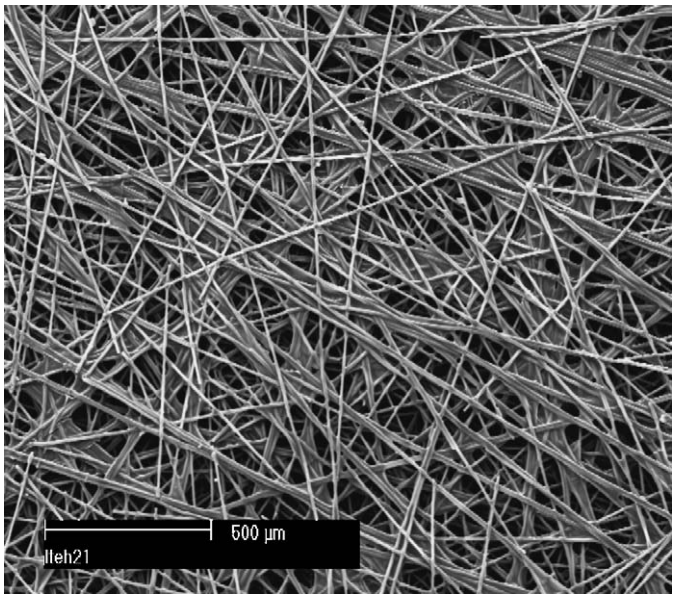

Fig. 4. Microscopic structure of carbon paper.

the anode to cathode results in a significant loss of fuel efficiency and reduction of the open circuit potential at the oxygen electrode. Two electrochemical reactions occur at the cathode side:

$$CH_3OH + H_2O \Rightarrow CO_2 + 6H^+ + 6e^- \quad (1)$$

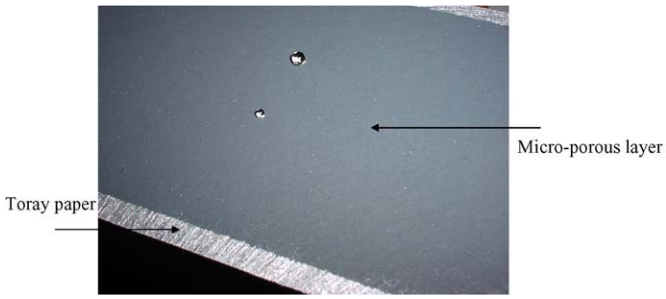

Fig. 5. Picture of carbon paper with a hydrophobic micro-porous layer.

$$\tfrac{3}{2}O_2 + 6H^+ + 6e^- \Rightarrow 3H_2O \quad (2)$$

As a result, the open circuit potential at cathode is a mixed potential, which can be expressed by:

$$E_c^{oc} = E_c^{mix} = E_c^{eq} - \eta_{cross}^{oc} \quad (3)$$

Here η_{cross}^{open} represents the cathode over potential produced by methanol crossover, which can be related to methanol flux as illustrated by the following:

$$6FJ_{cross} = i_{cross} = i_c^0 \exp\left(-\frac{\alpha_c F}{RT}\eta_{cross}^{oc}\right) \quad (4)$$

where J_{cross}, i_{cross}, i_c^0 and α_c represent methanol crossover flux, methanol crossover current density, exchange current density of the cathode, and cathodic transfer coefficient of the cathode, respectively.

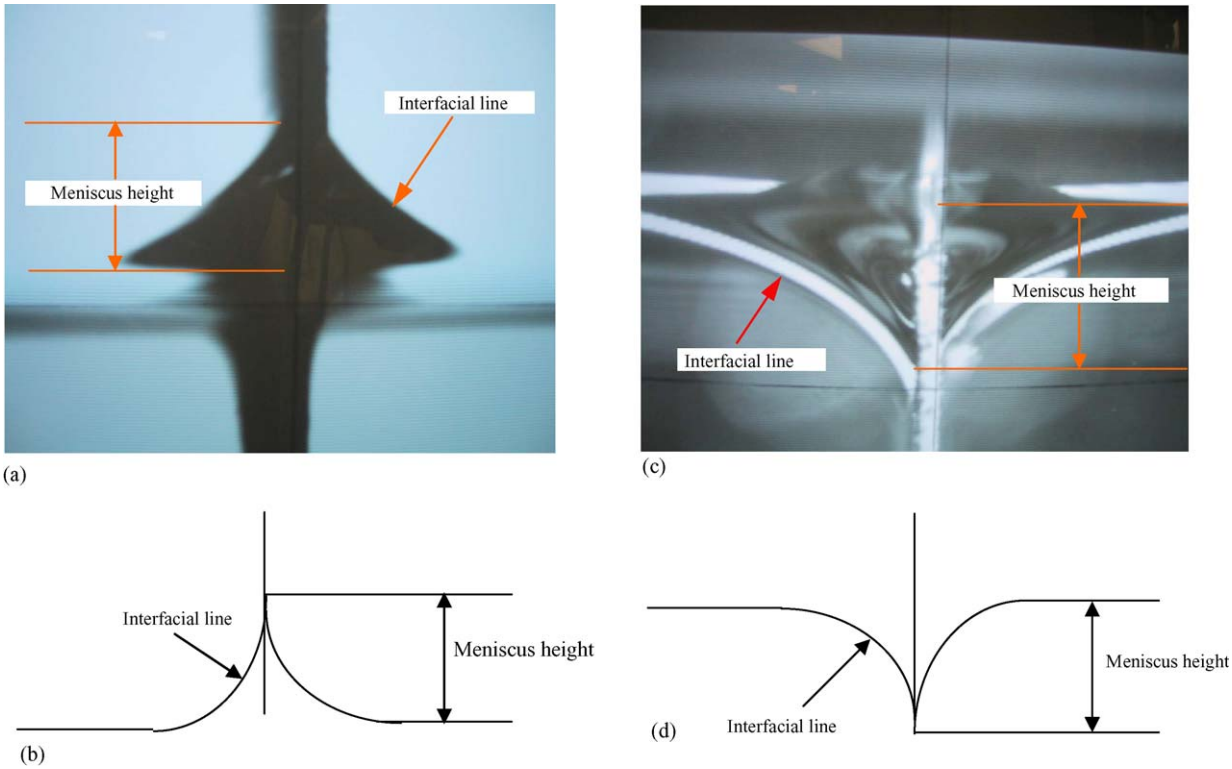

Fig. 6. Meniscus shape on different backing layers: (a) carbon cloth, (b) schematic diagram of meniscus shape on hydrophilic materials, (c) carbon paper with a micro-porous layer, and (d) schematic diagram of meniscus shape on hydrophobic materials.

Across the membrane, methanol transport is driven only by concentration gradients and electro-osmosis. At steady state, the mass transfer flux relation between different layers can be written as [7,9]:

$$\frac{i_{\text{cross}}}{6F} = D_{\text{b,eff}}^{\text{MeOH}} \frac{c^{0,\text{MeOH}} - c_{\text{c}}^{\text{MeOH}}}{l_{\text{b}}} - \frac{i}{6F}$$

$$= D_{\text{m,eff}}^{\text{MeOH}} \frac{C_{\text{c}}^{\text{MeOH}}}{l_{\text{m}}} + n_{\text{d}} \frac{i}{F} \quad (5)$$

From above equation, it can be seen that both diffusion and electro-osmotic drag contribute the total methanol crossover current density. When the methanol concentration in the anode catalyst layer drops to zero, the electrochemical reaction is totally controlled by methanol transport. The current density at this condition is defined as the anode limiting current density, which can be determined from Eq. (5) as:

$$i_{\text{lim}} = 6Fc^0 \frac{D_{\text{b,eff}}^{\text{MeOH}}}{1_{\text{b,eff}}} \quad (6)$$

At the limiting current density, there is no methanol crossover current because methanol concentration in the anode catalyst layer is equal to zero. Thus, this current density is only related to backing layer properties. At the open circuit, the crossover current density $i_{\text{cross}}^{\text{oc}}$ is only determined by methanol diffusion across backing layer and membrane layer. Therefore, Eq. (5) can be simplified as:

$$\frac{i_{\text{cross}}^{\text{oc}}}{6F} = D_{\text{b,eff}}^{\text{MeOH}} \frac{c^{0,\text{MeOH}} - c_{\text{c}}^{\text{MeOH}}}{l_{\text{b}}} = D_{\text{m,eff}}^{\text{MeOH}} \frac{c_{\text{c}}^{\text{MeOH}}}{l_{\text{m}}} \quad (7)$$

$i_{\text{cross}}^{\text{oc}}$ can be related to i_{lim} as [7]:

$$i_{\text{cross}}^{\text{oc}} = \frac{l_{\text{lim}}}{1 + (D_{\text{b,eff}}^{\text{MeOH}} l_{\text{m}} / D_{\text{m,eff}}^{\text{MeOH}} l_{\text{b}})} \quad (8)$$

If the electro-osmosis effect is not important, the flowing expression can be obtained [7,9]:

$$i_{\text{cross}} = i_{\text{cross}}^{\text{oc}} \left(1 - \frac{i}{i_{\text{lim}}}\right) \quad (9)$$

3.2. Cell performance comparison

A commercially available MEA made by Lynntech was procured for comparisons with the in-house MEA featuring a modified anode backing (Figs. 4 and 5). The Lynntech MEA also used a Nafion® 112 membrane, but its anode backing is commonly untreated carbon cloth. The wetting property of this carbon cloth can be seen in Fig. 6(a). After a piece of carbon cloth was dipped into a meniscus pool by using a micrometer-driven horizontal translator, the meniscus height was recorded by a charge coupled device (CCD) camera. An interfacial line between water, carbon cloth, and air can be observed. The positive meniscus height which is higher than the water pool level illustrates the hydrophilic surface. Aqueous solutions can easily penetrate this layer. In contrast, Fig. 6(b) displays the image of the in-house carbon paper backing layer in the same water pool. The negative meniscus height shows the hydrophobicity of its surface. The contact angle between water and tested specimen can be calculated by the following Eq. (10):

$$\theta = \sin^{-1}\left(1 - \frac{\Delta\rho g h^2}{2\sigma}\right) \quad (10)$$

It should be noted that the advanced contact angle θ_{a} typically is not equal to the recede contact angle θ_{r}, which means that the system exhibits contact angle hysteresis.

The different cell performance between the in-house MEA and Lynntech MEA with different anode backing layers is clearly seen in Fig. 7(a), where the cell was operated at 90 °C with 1.5 M methanol solution. At the same operation current density, the cell voltage with carbon paper plus micro-porous layer is higher than that of the cell with untreated carbon cloth. The voltage difference results in the higher power density of the cell with the modified anode backing. There is no limiting current at the

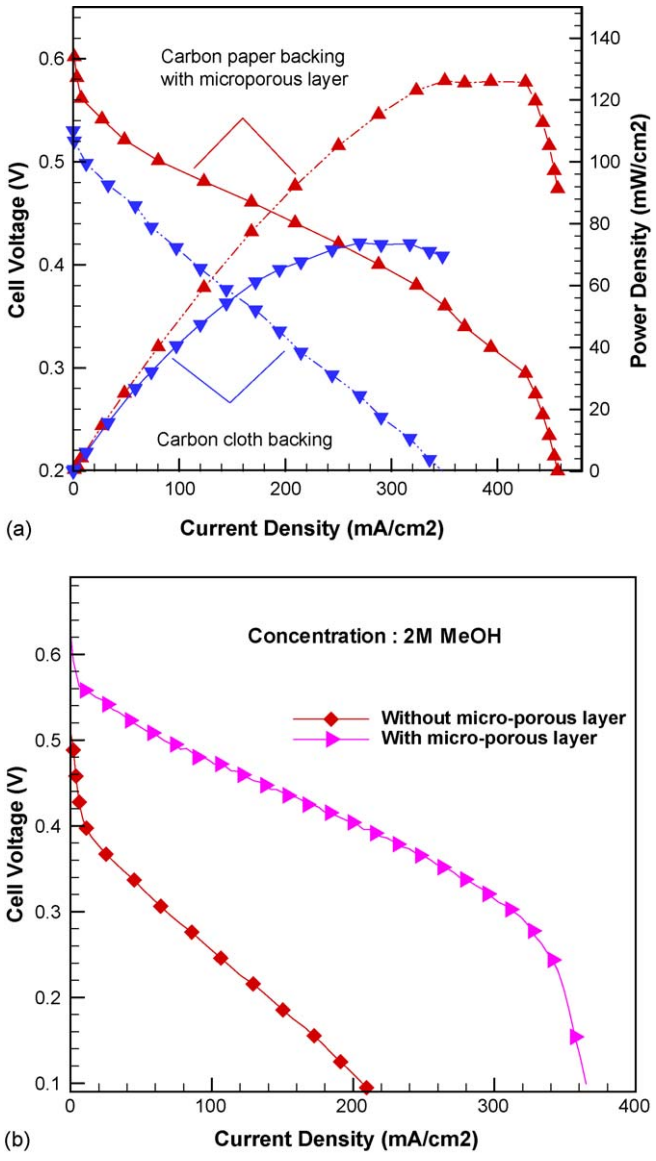

Fig. 7. Active DMFC polarization curve with different backing layers: (a) carbon cloth and carbon paper with micro-porous layer (90 °C, 1.5 M MeOH), (b) carbon paper with/without micro-porous layer.

0.1 V cutoff cell voltage for the Lynntech MEA. This behavior demonstrates that the conventional backing layer cannot limit methanol transport, which results in a higher methanol crossover rate. This can also be found from the lower open circuit potential. The data show that slowing methanol transport in the backing layer can benefit cell performance, which suggests that optimization of backing layer structure is necessary to control the proper methanol transport rate. Performance of the MEA with/without the micro-porous layer on the anode side was measured as well. The other fabrication methods used were the same. The backing layer effect on cell performance is shown in Fig. 7(b). It is obvious that the shape of the curve without the micro-porous layer is similar to that of Lynntech's MEA without the micro-porous layer. It can be found that the open circuit potential of the MEA without a micro-porous layer is nearly 0.1 V lower than that of the MEA with a micro-porous layer. Due to the utilization of the same cathode, the lower open circuit potential can rationally be attributed to the higher methanol crossover rate. It can also be seen that the cell potential of the MEA with a micro-porous layer (at the same current density) is higher than that of the MEA without a micro-porous layer. Furthermore, there is no appearance of a limiting current density in the polarization curve for the MEA without a micro-porous layer. These results show that, in order to optimize the performance of direct methanol fuel cells, it is valuable to add a micro-porous layer to reduce the impact of methanol crossover.

Methanol concentration could cause more effects on performance of the cell under air-breathing cathode condition; an experimental study under different concentrations is necessary to optimize the cell performance. Settings at a higher temperature result in an increase of the anode and the cathode reaction kinetics. Conversely, methanol crossover does

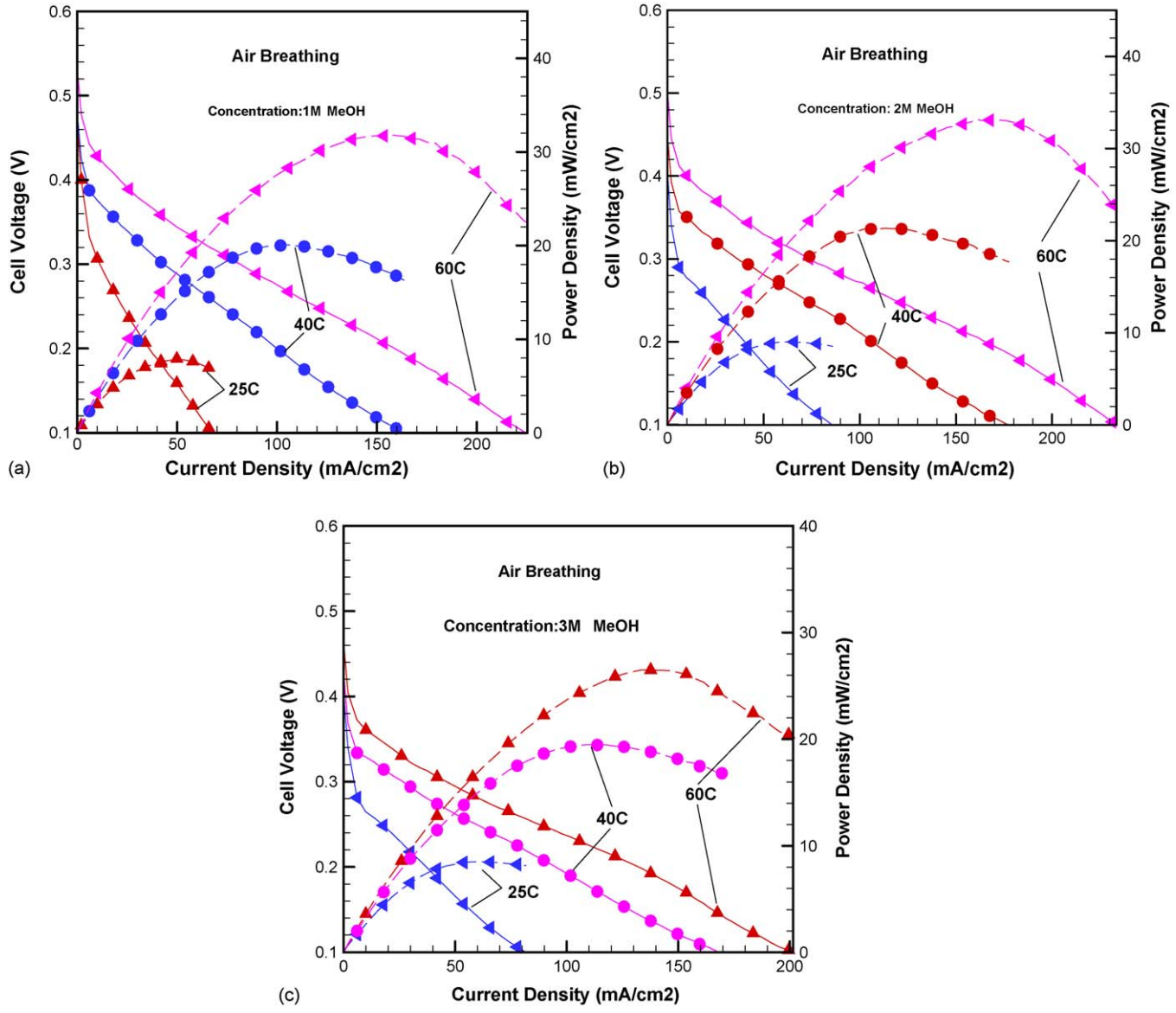

Fig. 8. Air-breathing DMFC polarization curve and power density with respect to current density with different MeOH concentrations (a Lytech MEA): (a) 1 M MeOH, (b) 2 M MeOH, and (c) 3 M MeOH.

increase with temperature and leads to a decrease in cell performance.

3.3. Temperature effects on cell performance

Temperature effects were examined as well. According to the above studies and previous investigations, the new MEAs were made with the cathode combined with a carbon cloth GDL and the in-house anode. As a comparison, a commercial MEA (purchased from Lynntech) with a hydrophilic anode side backing layer and a hydrophobic carbon cloth GDL was also examined (results in Fig. 8). At the same temperature, the open circuit potential decreases with the enhancement of the methanol concentration. As discussed before, the open circuit potential is not the equilibrium potential but a mixed potential, which can be written with the following:

$$E_c^{oc} = E_c^{eq} - \eta_c^{oc} \tag{11}$$

$$\eta_{cross}^{oc} = \frac{2.303RT}{\alpha_c F}\log\frac{i_{cross}}{i_0^{O_2}} \tag{12}$$

Combining Eqs. (11) and (12), the open circuit potential of the cathode E_c^{oc} can be related to methanol crossover density i_{cross} and the exchange current density of oxygen reduction reaction $i_0^{O_2}$ by:

$$E_c^{oc} = E_c^{eq} - \frac{2.303RT}{\alpha_c F}\log\frac{i_{cross}}{i_0^{O_2}} \tag{13}$$

Higher methanol concentration results in increased methanol crossover (an amplified methanol crossover current). Thus, it can be seen that the cathode potential decreases with the growing methanol crossover current according to the Eq. (13). As the operating temperature increases, the methanol crossover current density grows because of an increase in the methanol diffusion flux, which results in the reduction of the cathode potential. On the other hand, the oxygen reduction reaction rate grows with

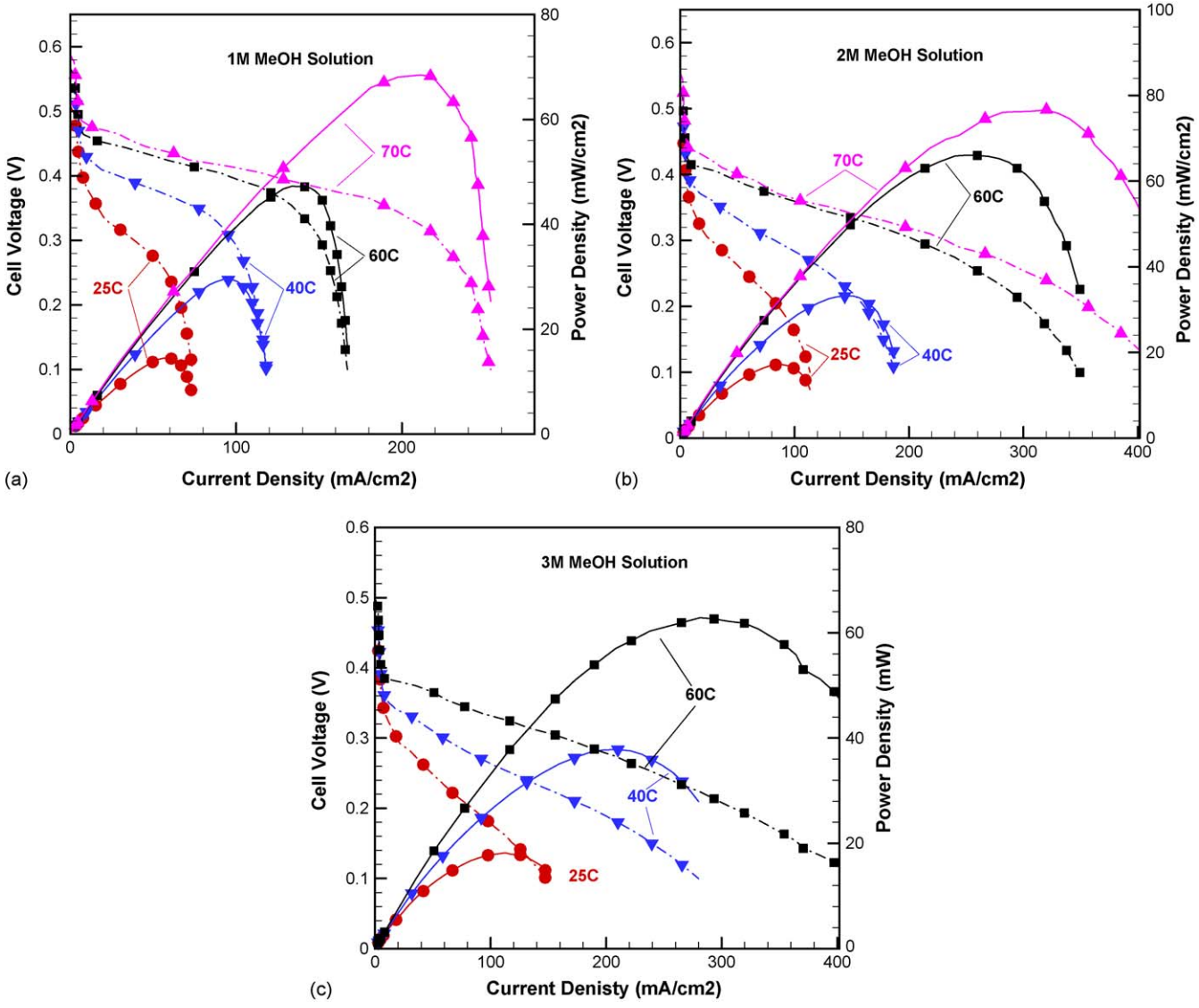

Fig. 9. Air-breathing DMFC polarization curve and power density with respect to current density with different MeOH concentrations (a new designed MEA): (a) 1 M MeOH, (b) 2 M MeOH, and (c) 3 M MeOH.

the development of temperature, which results in the increase of the cathode potential. The open circuit potential is controlled by oxygen reduction reaction kinetics and the methanol crossover rate. In these three figures, it can be found that all open circuit potentials rise as the operating temperature increases. This shows that the growth of potential due to increasing reaction rate is dominant although methanol crossover also enhance with the growth of temperature. The power densities of a fuel cell operating with three methanol concentrations are similar: about 10 mW cm^{-2} at 25 °C, 20 mW cm^{-2} at 40 °C, and 30 mW cm^{-2} at 60 °C. There is no water droplet observed visually at the GDL surface. It can be seen that there is no quick drop of cell voltage with respect to current density, which means there is no methanol transport limiting current density. Anode mass transport is not the limiting step.

The new designed MEA performance is shown in Fig. 9. All open circuit potentials are lower than in forced convection mode with backing pressure 15 psi (Fig. 10). The open circuit tendency for different temperatures and methanol concentrations are the same as the MEA purchased from Lynntech. The higher oxygen concentration resulting from backing pressure at the catalyst layer/GDL interface accounts for the higher potentials. Although all power densities at 25 °C are about 18 mW cm^{-2}, the voltage at the peak power is nearly at the cutoff voltage (0.1 V) for operating with a 3 M methanol solution, close to half of the other two voltages at the peak power. At 40 °C, the power densities operating with 1 and 2 M methanol solutions are over 20 mW cm^{-2} with a cell potential about 0.3 V, which is the output potential in practical applications. At 60 °C, maximum power density is about 65 mW cm^{-2}, this is more than half of the maximum power density for the forced convection fuel cell. It is found that methanol limiting current density appears when operating with 1 M and 2 M methanol solutions. At the knee point of a polarization curve, the power density achieves the peak value. It is important to operate fuel cells close to the knee point because methanol is mainly oxidized at the anode. It seems that a 2 M methanol solution is the best concentration for the air-breathing applications. It was found that a water droplet appeared at the surface of the cathode at a high current density.

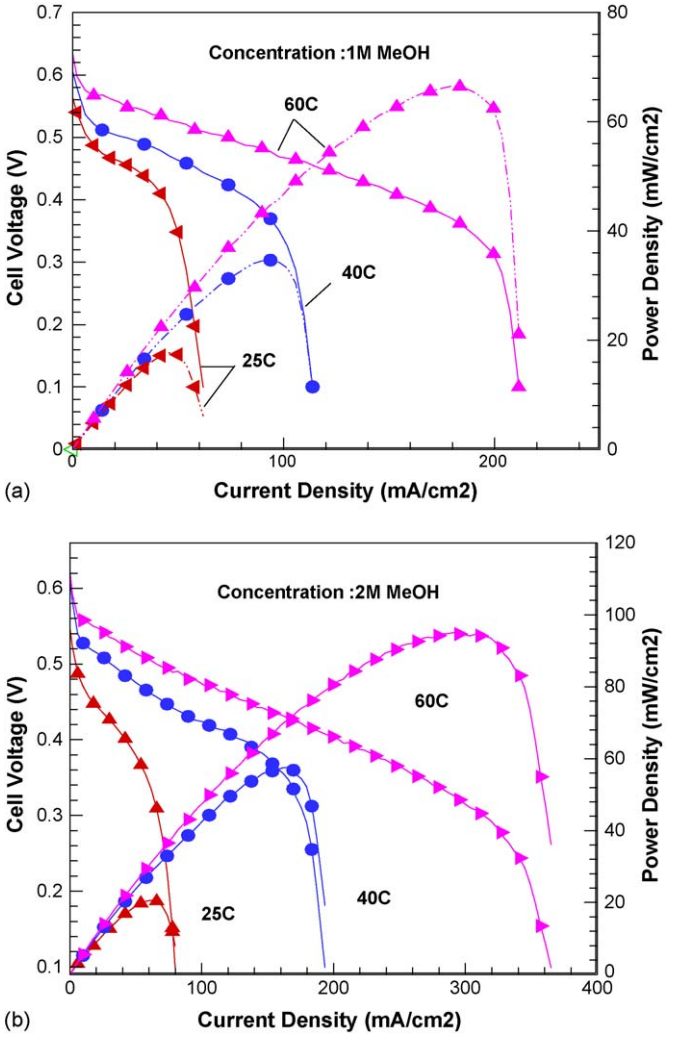

Fig. 10. Active DMFC polarization curve and power density with respect to current density with different MeOH concentrations (at a flow rate 10 ml s^{-1} with the backpressure 15 psi): (a) 1 M MeOH and (b) 2 M MeOH.

4. Conclusion

A novel MEA for an air-breathing DMFC was fabricated based on the previous investigation. It is demonstrated that the peak power of an advanced air-breathing DMFC is as twice as much as the peak power of a commercial DMFC obtained from Lynntech. It is found that the performance of the cell with 2 M methanol solution is the best. At 60 °C, a maximum power density 65 Mw cm^{-2} is achieved.

Acknowledgement

The author would like to thank Dr. Chao-Yang Wang of The Pennsylvania State University for helpful discussion and support.

Appendix A

The electrochemical reactions occurring in the DMFC can be written as follows:

$$\text{Anode}: CH_3OH + H_2O \Rightarrow CO_2 + 6H^+ + 6e^- \quad (A.1)$$

$$\text{Cathode}: \tfrac{3}{2}O_2 + 6H^+ + 6e^- \Rightarrow 3H_2O \quad (A.2)$$

$$\text{Overall reaction}: \tfrac{3}{2}O_2 + CH_3OH \Rightarrow CO_2 + 2H_2O \quad (A.3)$$

The standard Gibbs free energy change ΔG° of the reaction (A.3) with respect to the standard hydrogen reference electrode reaction can be calculated from thermodynamic data [11]:

$$-\Delta G^\circ = \Delta G^{\mathrm{f}}_{CO_2} - \Delta G^{\mathrm{f}}_{CH_3OH} - \Delta G^{\mathrm{f}}_{H_2O} \quad (A.4)$$

$$\Delta G^\circ (\mathrm{kJ\,mol^{-1}}) = -394.4 + 166.3 + 237.1 = 9.0 \quad (A.5)$$

Thus, the anode standard potential can be determined by:

$$E^\circ_{\mathrm{a}} = \frac{-\Delta G^\circ_{\mathrm{a}}}{6F} = \frac{9.0\times10^3}{6\times 96485} = 0.016\,\mathrm{V} \quad \text{versus} \quad \mathrm{SHE} \quad (A.6)$$

The standard Gibbs free energy change ΔG_c° of cathode reaction can be found by:

$$-\Delta G_c^\circ = 3\Delta G_{H_2O}^f = 3 \times 237.1 = 711.3(\text{kJ mol}^{-1}) \quad (A.7)$$

This leads to the cathode standard potential:

$$E_c^\circ = \frac{-G_c^\circ}{6F} = \frac{711.3 \times 10^3}{6 \times 96485} = 1.229\,\text{V} \quad \text{versus} \quad \text{SHE} \quad (A.8)$$

The overall cell equilibrium standard electromotive force (emf) can be determined:

$$\begin{aligned} E_{eq}^\circ &= -\frac{\Delta G^\circ}{nF} = -\frac{\Delta G_{CO_2}^f + 2\Delta G_{H_2O}^f - \Delta G_{CH_3OH}^f}{6F} \\ &= \frac{702.3 \times 10^3}{6 \times 96485} = 1.213\,\text{V} = E_c^0 - E_a^0 \\ &= 1.229 - 0.016 = 1.213\,\text{V} \end{aligned} \quad (A.9)$$

This value is extremely close to the theoretical cell voltage of a hydrogen proton exchange membrane fuel cell.

$$\begin{aligned} \Delta H^\circ &= \Delta H_{CO_2}^f + 2\Delta H_{H_2O}^f - \Delta H_{CH_3OH}^f \\ &= -393.5 - 2 \times 285.8 + 238.7 = -726.4\,\text{kJ} \end{aligned} \quad (A.10)$$

$$\eta_{eff} = \frac{\Delta G^\circ}{\Delta H^\circ} \times 100\% = \frac{702.3}{726.4} \times 100\% = 96.7\% \quad (A.11)$$

From Eq. (A.11), it can be seen that DMFC systems which do not follow Carnot's theorem, can produce electrical energy with theoretical thermodynamic efficiency close to 100%.

References

[1] K. Scott, W.M. Taama, P. Argyropoulos, J. Appl. Electrochem. 28 (1998) 1389.
[2] P. Argyropoulos, K. Scott, W.M. Taama, Electrochim. Acta 45 (2000) 1983.
[3] K. Scott, P. Argyropoulos, P. Yiannopoulos, W.M. Taama, J. Appl. Electrochem. 31 (2001) 823.
[4] E. Gülzow, T. Kaz, R. Reissner, H. Sander, L. Schilling, M.V. Bradke, J. Power Sources 105 (2002) 261.
[5] X. Ren, M.S. Wilson, S. Gottesfeld, J. Electrochem. Soc. 143 (1996) L12.
[6] A.K. Shukla, P.A. Christensen, A. Hamnett, M.P. Hogarth, J. Power Sources 55 (1995) 87.
[7] Y.H. Pan, Ph.D. dissertation, The Pennsylvania State University, 2004.
[9] Y.H. Pan, J. Electrochem. Soc., submitted for publication.
[11] R.J. Silbey, R.A. Alberty, Physical Chemistry, John Wiley & Sons, Inc., New York, 2001.